Available online at www.sciencedirect.com

ScienceDirect

www.elsevier.com/locate/jes

JES JOURNAL OF ENVIRONMENTAL SCIENCES

www.jesc.ac.cn

Hygroscopic properties of sodium and potassium salts as related to saline mineral dusts and sea salt aerosols

Huanhuan Zhang[1,3], *Wenjun Gu*[1,3], *Yong Jie Li*[2,*], *Mingjin Tang*[1,3,4]

[1] *State Key Laboratory of Organic Geochemistry and Guangdong Key Laboratory of Environmental Protection and Resources Utilization, Guangzhou Institute of Geochemistry, Chinese Academy of Sciences, Guangzhou 510640, China*

[2] *Department of Civil and Environmental Engineering, Faculty of Science and Technology, University of Macau, Avenida da Universidade, Taipa, Macau, China*

[3] *University of Chinese Academy of Sciences, Beijing 100049, China*

[4] *Center for Excellence in Regional Atmospheric Environment, Institute of Urban Environment, Chinese Academy of Sciences, Xiamen 361021, China*

ARTICLE INFO

Article history:
Received 11 September 2019
Revised 8 February 2020
Accepted 17 March 2020
Available online 9 April 2020

Keywords:
Sodium
Soil
Potassium
Hygroscopicity
Sea salt
Dust

ABSTRACT

Mineral dust, soil, and sea salt aerosols are among the most abundant primary inorganic aerosols in the atmosphere, and their hygroscopicity affects the hydrological cycle and global climate. We investigated the hygroscopic behaviors of six Na- and K-containing salts commonly found in those primary organic aerosols. Their hygroscopic growths as a function of relative humidity (RH) agree well with thermodynamic model prediction. Temperature dependence of deliquescence RH (DRH) values for five of those salts was also investigated, which are comparable to those in literature within 1%–2% RH, most showing negative dependence on temperature. Hygroscopic growth curves of real-world soil and sea salt samples were also measured. The hygroscopic growths of two more-hydroscopic saline soil samples and of sea salt can be predicted by the thermodynamic model based on the measured water-soluble ionic composition. The substantial amounts of water-soluble ions, including Na^+ and K^+, in saline soil samples imply that even nascent saline soil samples are quite hygroscopic at high-RH (>80%) conditions. For three less-hygroscopic dust samples, however, measurements showed higher water uptake ability than that predicted by the thermodynamic model. The small amount of water taken up by less-hygroscopic dust samples suggests that dust particles might contain thin layers of water even to very low RH. The results of this study provide a comprehensive characterization of the hygroscopicity of Na- and K-containing salts as related to their roles in the hygroscopic behaviors of saline mineral dusts and sea salt aerosols.

* Corresponding author.
E-mail: yongjieli@um.edu.mo (Y.J. Li).

https://doi.org/10.1016/j.jes.2020.03.046
1001-0742/

Introduction

Mineral dust and sea salt aerosols are among the most abundant primary inorganic aerosols in the atmosphere (ODowd et al., 1997; Jaegle et al., 2011; Tang et al., 2016, 2017; Wang et al., 2017; Zieger et al., 2017; Ibrahim et al., 2018). Physicochemical properties such as hygroscopicity of these types of primary inorganic aerosols have strong influence on hydrological cycle and global climate (Tang et al., 2019a), because those aerosols can serve as cloud condensation nuclei (CCN) or ice-nucleating particles (INP) (Connolly et al., 2009; Kumar et al., 2011; Prather et al., 2013; Karydis et al., 2017). Although most freshly emitted mineral dusts are considered as non-hygroscopic (Sullivan et al., 2009), a particular type, saline mineral dusts that contain appreciable amounts of soluble ions, can be hygroscopic (Koehler et al., 2007). On the other extreme, sea salt aerosols are highly hygroscopic because the dominating components are highly soluble electrolytes such as chloride (Cl^-, >50% by mass) and sodium (Na^+, >30% by mass) ions. Saline mineral dusts also contain substantial amounts of soluble electrolytes such as Na^+, potassium (K^+), and magnesium (Mg^{2+}). We have recently investigated the hygroscopic behaviors of calcium- and magnesium-containing salts (Guo et al., 2019). To better understand the hygroscopicity of saline mineral dusts and sea salt aerosols, it is essential to systematically investigate the hygroscopic behaviors of alkaline salts such as those of Na- and K-containing ones.

Many studies have been conducted for the hygroscopic behaviors of NaCl (Cohen et al., 1987; Richardson and Snyder, 1994; Cziczo et al., 1997; Lee and Hsu, 2000; Liu et al., 2008; Ahn et al., 2010; Schindelholz et al., 2014) and KCl (Cohen et al., 1987; Freney et al., 2009; Ahn et al., 2010; Li et al., 2014), or their mixtures (Li et al., 2014) and mixtures with other components (Hansson et al., 1998; Gupta et al., 2015). Li et al. (2017) summarized the deliquescence relative humidity (DRH) and efflorescence relative humidity (ERH) of a number of Na- and K-containing salts as related to the phase states. It was generally found that both NaCl and KCl deliquesce at medium-high RH (~75% and ~85% at 298 K, respectively); efflorescence occurs for these two salts at medium-low RH (~45% and ~60% at 298 K, respectively). In addition to association with halides such as chloride, sodium and potassium can also be associated with other anions such as sulfate (SO_4^{2-}) and nitrate (NO_3^-), due to processes such as heterogeneous reactions (Tang et al., 2017). The hygroscopicity of the salts with the latter two anions, however, remains relatively less investigated (Li et al., 2017). Uncertainty exists regarding the hygroscopicity of certain salts of sodium and potassium. For example, the presence of a hydrate form for Na_2SO_4 ($Na_2SO_4{\cdot}10H_2O$) can result in two distinct DRH values (85% and 93%) for this particular salt (Martin, 2000); there are conflicting results in literature regarding whether $NaNO_3$ effloresces or not (Richardson and Snyder, 1994; Tang and Munkelwitz, 1994; Lamb et al., 1996). Both hydration (water uptake and deliquescence) and dehydration (water loss and efflorescence) are important hygroscopic properties of mineral and soil materials. The ability to absorb and hold up water for mineral and soil materials, which is the focus of the current study, is particularly important in the enhanced light scattering (Martin, 2000) for aerosol particles and in the immobilization of liquid water in hyper-arid environments (Jia et al., 2018) for soils. The hygroscopic behaviors for multi-component mixtures are even more complex, with eutonic composition showing mutual DRH or ERH (Wexler and Seinfeld, 1991; Li et al., 2014). Mineral dust and sea salt aerosols are mixtures of multi-component salts, together with water-insoluble components. Therefore, it is important to measure the hygroscopicity of real-world samples to better understand their impacts on hydrological cycle and global climate.

In this work, we present hygroscopic growth measurements of six Na- and K-containing salts, including NaCl, $NaNO_3$, Na_2SO_4, KCl, KNO_3, and K_2SO_4. Comparisons between hygroscopic growth curves and those obtained from a thermodynamic model (ISORROPIA II) are made. Temperature-dependent (from 15 to 35°C) DRH values are also presented. Hygroscopic growths for real-world samples, including five soil samples, two of which are saline soils, and one sea salt sample, are also presented. Ionic composition of real-world samples were used to model the hygroscopic growths, which are then compared to those measured. Discussion on discrepancies observed, if any, is also provided. Although only limited to hydration and deliquescence behaviors, the present study provides a comprehensive data set for hygroscopicity of Na- and K-containing salts, which is useful for understanding the climate effects of mineral dusts and sea salt aerosols.

1. Materials and methods

1.1. Chemicals and soil/sea salt samples

Sodium chloride (NaCl, >99.5%), potassium chloride (KCl, >99.5%) and potassium sulfate (K_2SO_4, >99%) were purchased from Aldrich. Sodium nitrate ($NaNO_3$, >99.99%), sodium sulfate (Na_2SO_4, >99%) and potassium nitrate (KNO_3, >99%) were supplied by Aladdin, Strem and Guangzhou Chemical Reagent Factory, respectively. These chemicals were used without further purification. Synthetic inorganic sea salt, which mimics water soluble inorganic composition of sea water, was provided by Himedia, Mumbai, India (Tang et al., 2019b). Five soil samples used in this work (GBW07447, GBW07448, GBW07449, GBW07450 and GBW07454) were supplied by Chinese Academy of Geological Sciences as certificated materials. The soil sample GBW07447 is saline-alkali soil from Hangjinhouqi, Inner Mongolia of China, GBW07448 is brown desert soil from Haiyan County, Qinghai Province of China, GBW07449 is saline-alkali soil from Shanshan County, Xinjiang of China, GBW07450 is sierozem from Shihezhi City, Xinjiang of China, and GBW07454 is loess from Luochuan County, Shanxi Province of China. Compositions of these soil samples, analyzed using ion chromatography, can be found elsewhere (Tang et al., 2019c).

1.2. Hygroscopic growth

A vapor sorption analyzer (Q5000SA, TA Instruments, USA) was used for the hygroscopic measurements. Detailed description of the instrument and the procedure has been provided in our previous study (Gu et al., 2017). The instrument contains (1) a high-precision balance that can measure mass change of <0.1 μg with an accuracy of ±0.1%, and (2) a humidity chamber that regulates RH between 0% to 98% with ±1% uncertainty and a temperature range of 5–85°C with ±0.1°C uncertainty. The dynamic range for mass measurement is 0–100 mg. At a stable temperature set point, samples of normally 1 – 10 mg were placed on the sample pan in the sample chamber, and RH was brought to 0%. The sample and reference chambers were then conditioned to stepwise increases of RH, with the mass change, RH value, and temperature continuously measured with a time resolution of 30 sec. If mass change is less than 0.1% in 30 min, equilibrium between water vapor and the sample is assumed, and the RH value in the chambers will be raised to another set point. Sample mass values of the last 30 min of each RH step were then averaged to be the mass of that RH condition. This average mass value is

normalized by the mass at lowest RH (0%) to obtain the mass growth factor (MGF).

We performed the thermodynamic model ISORROPIA II (Nenes et al., 1998; Fountoukis and Nenes, 2007) based on the molar contributions for the ions measured, assuming that the rest of the sample is non-hygroscopic. The ISORROPIA II model was run for a temperature of 298 K in the "forward" mode, with solid formation allowed.

1.3. *DRH determination*

The procedure of DRH determination has also been detailed in our previous study (Gu et al., 2017). Briefly, the sample was first dried at 0% RH until mass change was less than 0.1% in 30 min. RH was then increased to about 5%–10% RH lower than the anticipated DRH value based on the hygroscopic growth curve as determined in the above experiments, and the sample was conditioned for 30 min. Then RH was increased stepwise by 1% increment. When a significant increase in sample mass was observed, that RH value was determined to be the DRH.

2. Results and discussion

2.1. *Hygroscopic growth*

Examples of hygroscopic growth measurements for NaCl and KCl at 25°C are shown in Fig. 1a and c. The panels show RH ramping programs and MGF values as a function of experimental time. For NaCl, the MGF remained close to unity when RH was up to 70%; by setting RH from 70% to 80%, the sample started to take up water and MGF grew substantially to 4.5; further increasing RH to 90% led to another stage of MGF from 4.5 to 7.2. For KCl, the jump of MGF occurred at 80%–90% RH. For both salts, after >5 hr of equilibration at the highest RH (90%), we brought the RH back to the driest state (0%). Water desorption was rapid, with MGF going back to unity within 30 min.

Hygroscopic growths for all six salts were investigated with at least duplicate measurements. Fig. 2 presents the MGF as a function of RH for the six salts. The hydration legs from the thermodynamic model ISORROPIA II (Nenes et al., 1998; Fountoukis and Nenes, 2007) were also presented in Fig. 2 for comparison. For all the six measured salts, the hygroscopic growths from our measurements agree well with the model prediction. This comparison gives us confidence that our measurement technique can provide reproducible hygroscopic growth results, which will later be used for real-world samples.

For NaCl (Fig. 2a), we had two data points above the DRH of this salt (~75%). For this reason, in the time series of MGF (Fig. 1a), we observed two equilibrated stages with substantial amounts of water uptake (80% and 90% RH). This is also the case for $NaNO_3$ (Fig. 2c). On the contrary, there was only one data point above DRH for KCl (Fig. 2b), and only one stage of equilibrated water uptake was observed in the time series of MGF as shown in Fig. 1c. This is also the case for Na_2SO_4. For KNO_3, the DRH is higher than 90%, we only observed water uptake at RH 95% as shown in Fig. 2d. For K_2SO_4, the DRH is higher than 95%, and water uptake was not observed in our experiments.

2.2. *Deliquescence RH*

Fig. 1b and d shows the typical experimental results in the determination of DRH values for NaCl and KCl, respectively. By starting at a lower RH value near the anticipated deliquescence point obtained from the hygroscopic growth measurements, small increments of 1% RH were used to condition the samples. At RH values where a rapid jump of MGF was observed, the DRH value for the sample was thus determined. Such jumps occurred at 75%–76% RH for NaCl and 84%–85% for KCl as shown in Fig. 1.

Table 1 lists the DRH values for five out of the six salts investigated in this study. At 25°C, the DRH values for NaCl, KCl, $NaNO_3$, KNO_3, and Na_2SO_4 are 75.1%, 84.1%, 73.5%, 92.5%, and 86.5%, respectively, in agreement with literature values (Greenspan, 1977) within 1%–2% RH. The DRH value of K_2SO_4 was not determined because it was higher than the maximum set RH (95%) in our experiments.

Temperature dependence of DRH values are also shown in Table 1. With increasing temperature from 15 to 35°C, DRH values of the five salts normally decreased, in agreement with literature (Greenspan, 1977), except for Na_2SO_4. This result suggests that dissolution of most of the Na- and K-containing salts investigated in our study is endothermic, with higher temperature favoring dissolution, thus deliquescence. The implication is that long-range transport of mineral dust particles containing these salts might make deliquescence of those dust particles easier. For example, if mineral dust particles, especially saline dust particles that contain sodium and potassium, are transported from the arid areas such as those in northwestern China to southeastern coastal regions, it is likely that deliquescence can occur more easily, because both RH and temperature are higher in the southeastern coastal regions. The potential presence of a mixture between anhydrous Na_2SO_4 and decahydrate ($Na_2SO_4{\cdot}10H_2O$) in the temperature range of our experiments (15–35°C) might be the reason behind the abnormal temperature dependence. Dissolution of Na_2SO_4 is endothermic, while that of its decahydrate is exothermic (Angeli et al., 2010; Bharmoria et al., 2014).

2.3. *Soil and sea salt samples*

To better understand the hygroscopic behaviors of Na- and K-containing mineral and sea salt samples, the hygroscopic growth of real-world samples were investigated as shown in Fig. 3. Two soil samples (GBW07447 and GBW07449) and the sea salt sample showed very high hygroscopicity, with the MGF value for sea salt sample being above 6 at 90% RH. On the contrary, the other three soil samples (GBW07448, GBW07450 and GBW07454) showed very low hygroscopicity, with their MGF values being less than 1.04 even at 90% RH. While GBW07447 and GBW07449 are both saline-alkaline soil samples, the sea salt is the sample contains the largest amount of water-soluble ions. The other three are, however, mineral dust samples that contain much lower contents of water-soluble ions (see below).

Water-soluble ionic composition of these soil and sea salt samples were then analyzed using ion chromatography, and their mass percentages and equivalent molar number (based on 100 g of sample) are listed in Table 2. For those more-hygroscopic samples, Na^+ and K^+ ions together with Mg^{2+} ions contributed significantly to the sample mass, with the balancing anion as mostly Cl^- or SO_4^{2-}. Specifically, water-soluble ions contributed to 4.8% and 21.2% of the total mass in soil samples GBW07447 and GBW07449, respectively. Over 99% of the sea salt sample is made up by water-soluble ions. For those less-hygroscopic soil samples, the water-soluble ionic composition is normally less than 1% by mass (Table 2). In addition, Table 2 also shows that for more-hygroscopic salts, the measured water-soluble cations were equal to or less than the measured water-soluble anions on an equivalent basis. The missing cation could potentially be NH_4^+, whose salts are mostly hygroscopic, that is not measured in our IC method. On the contrary, for less-hygroscopic salts, the measured water-soluble cations were much more than the measured water-soluble anions on an equivalent basis. The missing anions

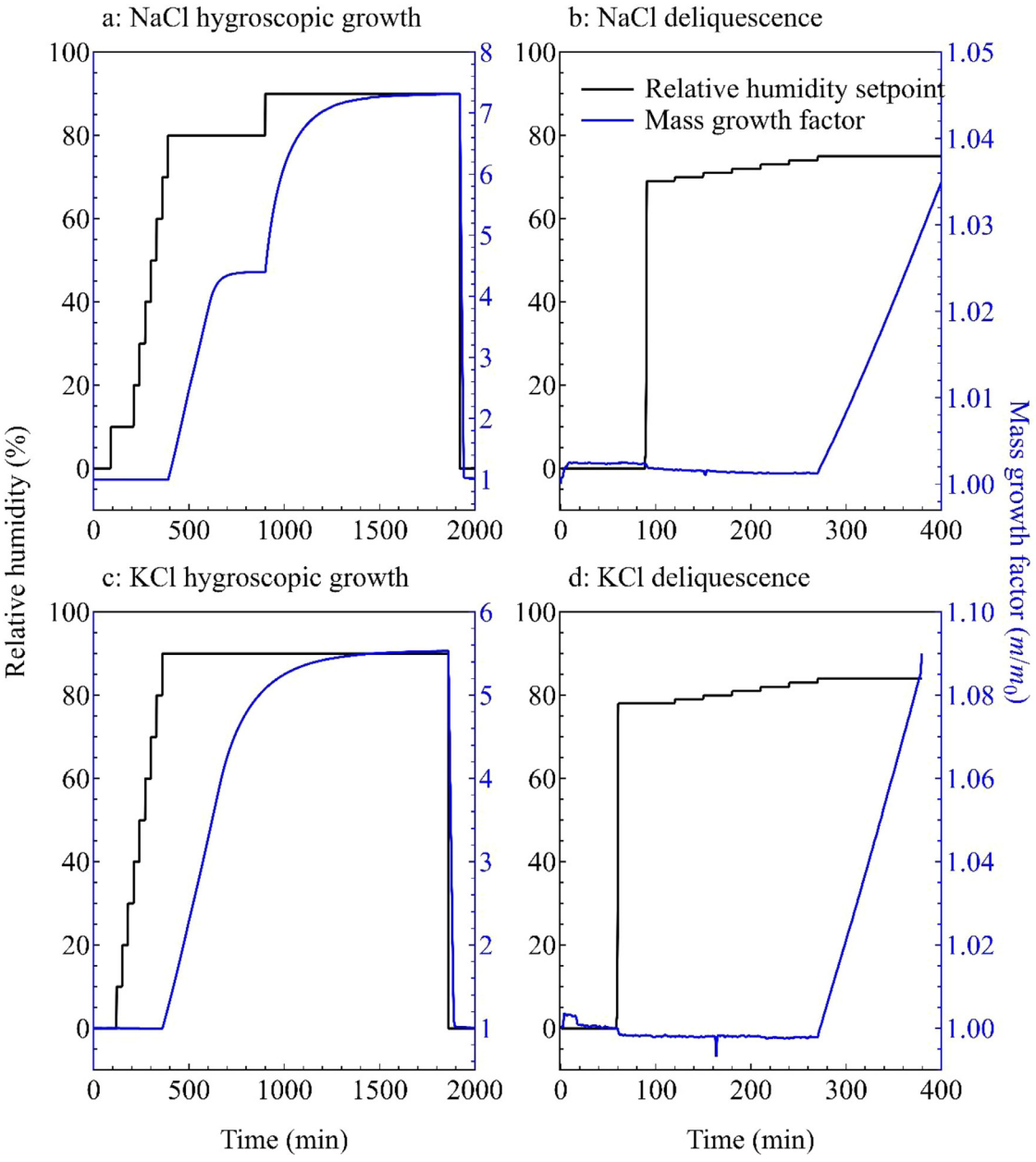

Fig. 1 – Examples of hygroscopic growth measurements: (a) for NaCl and (c) for KCl, and DRH determination measurements: (b) for NaCl and (d) for KCl.

could potentially be some organic acids that were not covered in our IC measurements. These missing anions might be the reason for the higher-than-predicted water uptake for the less-hygroscopic salts, as discussed below. Therefore, Na- and K-containing salts, together with Mg-containing ones, play a vital role in the hygroscopic water uptake for mineral dusts. For these nascent soil and sea salt samples, the mass fractions of NO_3^- are very low (<0.1%). These low fractions of nitrate in the real-world samples investigated contributed little to the overall hygroscopicity. Aged mineral dust or sea salt aerosols, however, can contain substantial amounts of nitrate due to heterogeneous reactions between gaseous nitrogenous species (e.g., HNO_3) and those aerosol particles (Tang et al., 2017). Given that nitrate salts are generally very hygroscopic (for instance, $NaNO_3$), the aged mineral dust particles would possess enhanced hygroscopicity.

We also performed thermodynamic prediction using ISORROPIA II to estimate the hygroscopic growths of those real-world samples, based on the contents of measured water-soluble ionic composition and assuming non-hygroscopic for the rest of their masses. As shown in Fig. 3, the model results match with experimental data quite well for more-hygroscopic samples, while the agreements were not satisfactory for less-hygroscopic ones. This result implies that the ionic composition as measured in our study can be used to predict hygroscopic behaviors of un-processed saline soil dust and sea salt aerosols. For those less-hygroscopic samples, however, the small amount of water uptake that could not be captured by model prediction using the water-soluble ions measured, and might be due to some water-soluble components in the samples that are not measured by our IC method (potentially organic acids). This small water uptake even to

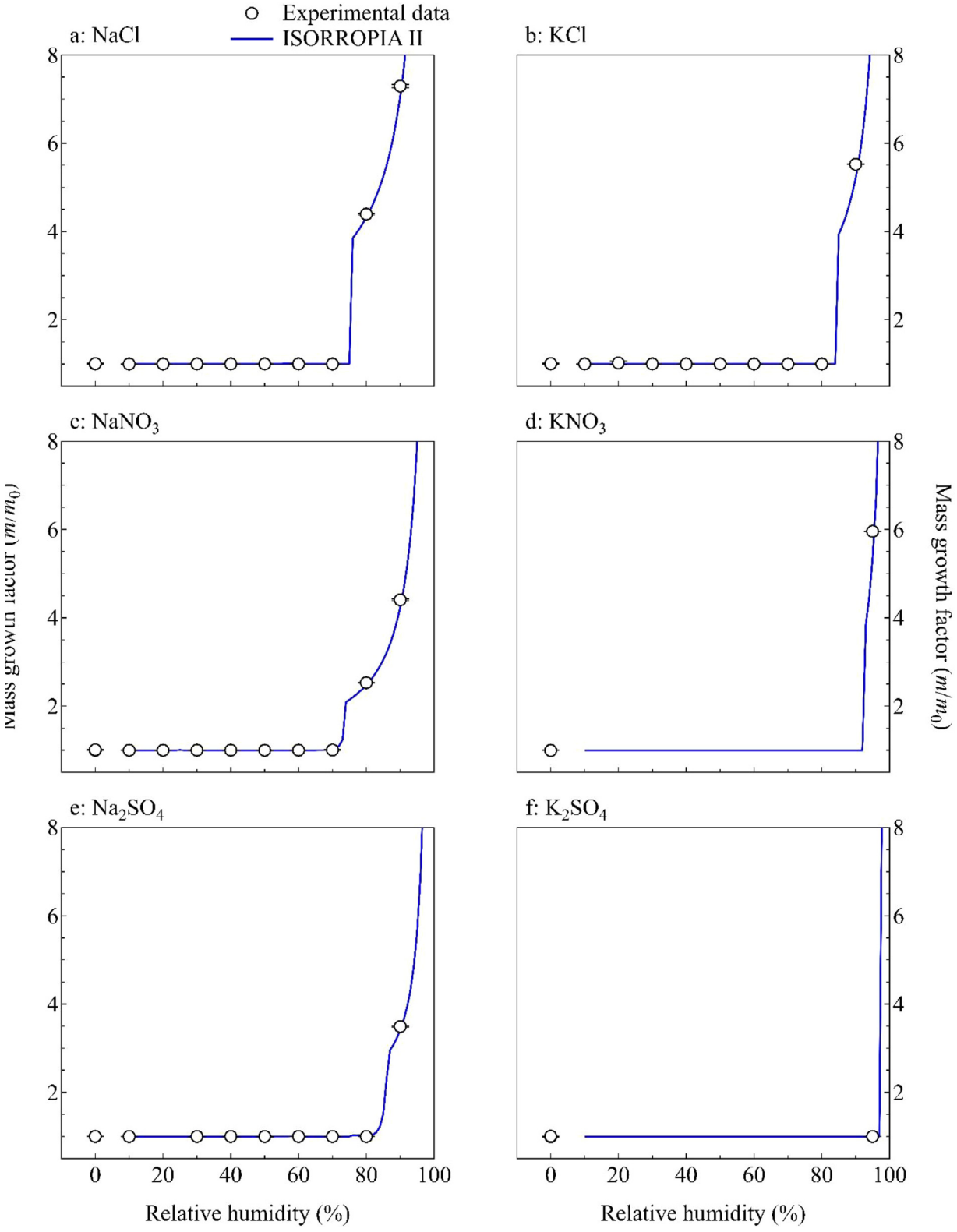

Fig. 2 – Hygroscopic growth of (a) NaCl, (b) KCl, (c) $NaNO_3$, (d) KNO_3, (e) Na_2SO_4, and (f) K_2SO_4, together with those from predictions with ISORROPIA II (Fountoukis and Nenes, 2007).

Table 1 – Comparison of deliquescence relative humidity (DRH) values measured in this study with those reported in literature (Greenspan, 1977) for NaCl, $NaNO_3$, Na_2SO_4, KCl, KNO_3, and K_2SO_4 from 15 to 35°C.

Salt	T (°C)	DRH	Reference (Greenspan, 1977)	Salt	T (°C)	DRH	Reference (Greenspan, 1977)
NaCl[a]	15	75.3 ± 1.2	75.6 ± 0.2	KCl[a]	15	85.5 ± 1.1	85.9 ± 0.3
	20	75.3 ± 1.1	75.5 ± 0.1		20	84.7 ± 1.1	85.1 ± 0.3
	25	75.1 ± 1.1	75.3 ± 0.1		25	84.1 ± 1.1	84.3 ± 0.3
	30	75.2 ± 1.0	75.1 ± 0.1		30	83.6 ± 1.0	83.6 ± 0.3
	35	75.0 ± 1.0	74.9 ± 0.1		35	83.0 ± 1.0	83.0 ± 0.3
$NaNO_3$	15	74.5 ± 1.0	76.5 ± 0.4	KNO_3	15	93.5 ± 1.0	95.4 ± 1.0
	20	74.5 ± 1.0	75.4 ± 0.4		20	93.5 ± 1.1	94.6 ± 0.7
	25	73.5 ± 1.0	74.3 ± 0.3		25	92.5 ± 1.0	93.6 ± 0.6
	30	72.5 ± 1.0	73.1 ± 0.3		30	91.5 ± 1.0	92.3 ± 0.6
	35	71.5 ± 1.0	72.1 ± 0.3		35	90.5 ± 1.0	90.8 ± 0.8
Na_2SO_4	15	84.5 ± 1.0	–	K_2SO_4	15	–	97.9 ± 0.6
	20	85.5 ± 1.0	–		20	–	97.6 ± 0.5
	25	86.5 ± 1.0	84.35 ± 0.5[b]		25	–	97.3 ± 0.5
	30	87.5 ± 1.0	–		30	–	97.0 ± 0.4
	35	88.5 ± 1.0	–		35	–	96.7 ± 0.4

[a] Average DRH values for NaCl and KCl were calculated by measurements (duplicate or triplicate) in this study and those reported in Gu et al. (2017). Uncertainties were calculated by taking into account of standard deviations in this study, 1% error in RH measurements, and the errors in Gu et al. (2017) with error propagation. Averages DRH values for other salts were from duplicate or triplicate measurements in this study, with errors propagated from the standard deviations and 1% error in RH measurements.

[b] Average and standard deviation from Tang et al. (1995), Lee and Hsu (1998), Lee and Chang (2002), and Feng et al. (2014).
-: not available; T: temperature.

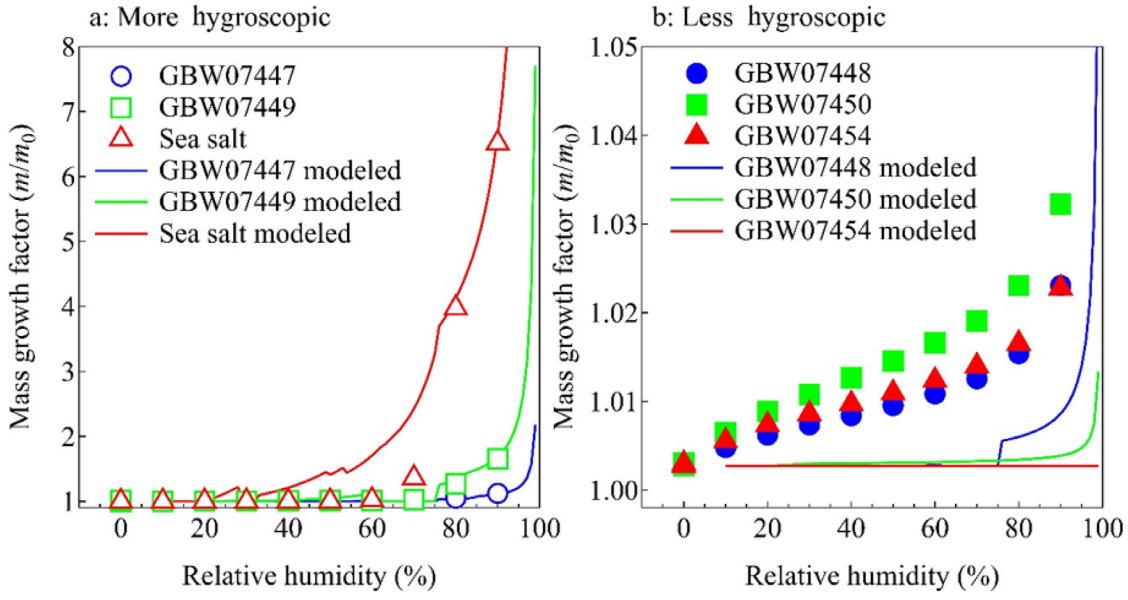

Fig. 3 – Hygroscopic growth of soil samples and sea salt sample: (a) more-hygroscopic samples; (b) less-hygroscopic samples.

very low RH, however, implies that a thin water layer can form on the surface of those less-hygroscopic mineral dust particles.

3. Conclusions and implications

We measured the hygroscopic growth curves of six typical Na- and K-containing salts, which agree well with thermodynamic model prediction. We also determined their DRH values, which are comparable to those in literature within 1%-2% RH. Temperature dependence of DRH values for five of those salts was also investigated. Four of the five salts showed decreased DRH values as temperature increased. The only exception was Na_2SO_4, which showed increased DRH values as temperature increased. This result suggests that the possible co-existence of anhydrous Na_2SO_4 and decahydrate ($Na_2SO_4{\cdot}10H_2O$) might have complicated temperature dependence of this particular salt. Hygroscopic growth curves of real-world soil and sea salt samples were also measured. The water uptake ability of two more-hygroscopic saline mineral samples and of sea salt can be predicted by the thermodynamic model based on the measured water-soluble ionic

Table 2 – Mass percentage and equivalent molar number (μeq (× 10^6), based on the same total mass of 100 g sample, taking into account of ion molecular weight and ion charge) of water-soluble inorganic ions in soil samples and sea salt sample.

	GBW07447		GBW07448		GBW07449		GBW07450		GBW07454		Sea salt	
	Mass (%)	μeq (× 10^6)	Mass (%)	μeq (× 10^6)	Mass (%)	μeq (× 10^6)	Mass (%)	μeq (× 10^6)	Mass (%)	μeq (× 10^6)	Mass (%)	μeq (× 10^6)
Na^+	1.11	4.82	0.08	0.37	6.09	26.49	0.10	0.46	0.02	0.10	30.8	133.91
K^+	0.07	0.32	0.07	0.32	0.15	0.66	0.08	0.35	0.06	0.26	1.0	4.35
Ca^{2+}	0.07	0.28	0.05	0.22	0.04	0.19	0.03	0.13	0.03	0.13	1.1	4.78
Mg^{2+}	1.20	5.20	0.74	3.22	2.37	10.30	0.60	2.62	0.71	3.08	3.7	16.09
NO_3^-	0.00	0.00	0.00	0.00	0.00	0.00	0.01	0.05	0.00	0.00	0.0	0.00
Cl^-	0.56	2.44	0.05	0.22	3.78	16.42	0.01	0.04	0.00	0.00	55.3	240.43
SO_4^{2-}	1.77	7.70	0.16	0.70	8.79	38.21	0.02	0.09	0.01	0.05	7.5	32.61
Others	95.2	2%[a]	98.8	64%[a]	78.8	-18%[a]	99.1	91%[a]	99.2	97%[a]	0.6	-26%[a]

GBW07447: saline-alkaline soil; GBW07448: brown desert soil; GBW07449: saline-alkaline soil; GWB07450: sierozem; GBW07454: loess.

[a] Percentage of ion imbalance: Imbalance = $100\% \times \frac{\sum \text{Cation equivalent molar number} - \sum \text{Anion equivalent molar number}}{\sum \text{Cation equivalent molar number} + \sum \text{Anion equivalent molar number}}$.

composition. For three less-hygroscopic dust samples, however, measurements show higher water uptake ability than that predicted by the thermodynamic model. This result suggests that a thin layer of water may exist even for those less-hygroscopic soil types due to the presence of components other than the inorganic salts measured. This finding implies that there is a small but not negligible ability to absorb water for less-hygroscopic soils in arid/hyper-arid environments, and that even less-hygroscopic soil/dust aerosol particles have the capability to provide an aqueous thin film for heterogeneous reactions.

We provide here a comprehensive characterization of hygroscopicity of Na- and K-containing salts and of real-world soil, dust and sea salt samples. The implications of the current study are several folds. First, most of the Na- and K-containing salts investigated in this study showed a decrease in DRH values as temperature increased, indicating easier deliquescence with higher temperature. In addition, together with a previous study (Tang et al., 2019c), we show that some saline-alkaline samples can be quite hygroscopic and has the capability to take up a substantial amount of water at high RH conditions. These results suggest that long-range transport of soil/dust particles to high-temperature and high-RH regions (e.g., in coastal areas or over the ocean) can make water uptake more easily. Upon water uptake on those soil/dust particles, surface water layer formation provides a venue for aqueous-phase reactions (Li et al., 2017; Jing et al., 2018). Furthermore, activation of those soil/dust particles into cloud droplets would also be easier compared to completely non-hydroscopic dust aerosols (Koehler et al., 2007). Second, the presence of substantial amounts of water-soluble ions in the saline mineral dusts is the reason behind their high hygroscopicity. Specifically, Na, K, and Mg cations and chloride and sulfate anions are found to be in high abundance for those hygroscopic soil samples. Interestingly, nitrate content in all of those soil samples was all less than 0.1%, indicating that the nascent soil/dust samples do not contain this particular anion. In processed dust/soil particles, however, nitrate can be present in a substantial amount by heterogeneous reactions with nitrogenous pollutants (Tang et al., 2017), and may alter the hygroscopicity of aged dust/soil particles. Further investigations are needed to ascertain the role of nitrate in aged dust/soil particles on their hygroscopicity.

Declaration of competing interest

None.

Acknowledgments

This work was funded by Ministry of Science and Technology of China (No. 2018YFC0213901), National Natural Science Foundation of China (Nos. 91744204 and 41675120), Guangdong Foundation for Program of Science and Technology Research (Nos. 2017B030314057 and 2019B121205006), the Science and Technology Development Fund, Macau SAR (No. 016/2017/A1) and the Multi-Year Research grant (No. MYRG2018-00006-FST) from the University of Macau. Yongjie Li would like to acknowledge Open Grant from State Key Lab of Organic Geochemistry Chinese Academy of Sciences. Mingjin Tang would like to thank the CAS Pioneer Hundred Talents program for providing a starting grant.

REFERENCES

Ahn, K.H., Kim, S.M., Jung, H.J., Lee, M.J., Eom, H.J., Maskey, S., et al., 2010. Combined use of optical and electron microscopic techniques for the measurement of hygroscopic property, chemical composition, and morphology of individual aerosol particles. Anal. Chem. 82, 7999–8009.

Angeli, M., Hebert, R., Menendez, B., David, C., Bigas, J.P., 2010. Influence of temperature and salt concentration on the salt weathering of a sedimentary stone with sodium sulphate. Eng. Geol. 115, 193–199.

Bharmoria, P., Gehlot, P.S., Gupta, H., Kumar, A., 2014. Temperature-dependent solubility transition of Na_2SO_4 in water and the effect of NaCl therein: solution structures and salt water dynamics. J. Phys. Chem. B 118, 12734–12742.

Cohen, M.D., Flagan, R.C., Seinfeld, J.H., 1987. Studies of concentrated electrolyte-solutions using the electrodynamic balance .1. Water activities for single-electrolyte solutions. J. Phys. Chem. 91, 4563–4574.

Connolly, P.J., Mohler, O., Field, P.R., Saathoff, H., Burgess, R., Choularton, T., et al., 2009. . Studies of heterogeneous freezing by three different desert dust samples. Atmos. Chem. Phys. 9, 2805–2824.

Cziczo, D.J., Nowak, J.B., Hu, J.H., Abbatt, J.P.D., 1997. Infrared spectroscopy of model tropospheric aerosols as a function of relative humidity: observation of deliquescence and crystallization. J. Geophys. Res. Atmos. 102, 18843–18850.

Feng, X.N., Chen, H.N., Luan, Y.M., Tan, S.H., Pang, S.F., Zhang, Y.H., 2014. In-situ FTIR-ATR spectroscopic observation on the dynamic efflorescence/deliquescence processes of Na_2SO_4 and mixed Na_2SO_4/glycerol droplets. Chem. Phys. 430, 78–83.

Fountoukis, C., Nenes, A., 2007. ISORROPIA II: a computationally efficient thermodynamic equilibrium model for K^+-Ca^{2+}-Mg^{2+}-NH_4^+-Na^+-SO_4^{2-}-NO^{3-}-C^{l-}-H_2O aerosols. Atmos. Chem. Phys. 7, 4639–4659.

Freney, E.J., Martin, S.T., Buseck, P.R., 2009. Deliquescence and efflorescence of potassium salts relevant to biomass-burning aerosol particles. Aerosol Sci. Technol. 43, 799–807.

Greenspan, L., 1977. Humidity fixed points of binary saturated aqueous solutions. J. Res. Natl. Bur Stand. A Phys. Chem. 81A, 89–96.

Gu, W.J., Li, Y.J., Zhu, J.X., Jia, X.H., Lin, Q.H., Zhang, G.H., et al., 2017. Investigation of water adsorption and hygroscopicity of atmospherically relevant particles using a commercial vapor sorption analyzer. Atmos. Meas. Tech. 10, 3821–3832.

Guo, L., Gu, W., Peng, C., Wang, W., Li, Y.J., Zong, T., et al., 2019. A comprehensive study of hygroscopic properties of calcium- and magnesium-containing salts: implication for hygroscopicity of mineral dust and sea salt aerosols. Atmos. Chem. Phys. 19, 2115–2133.

Gupta, D., Eom, H.J., Cho, H.R., Ro, C.U., 2015. Hygroscopic behavior of NaCl-$MgCl_2$ mixture particles as nascent sea-spray aerosol surrogates and observation of efflorescence during humidification. Atmos. Chem. Phys. 15, 11273–11290.

Hansson, H.C., Rood, M.J., Koloutsou-Vakakis, S., Hameri, K., Orsini, D., Wiedensohler, A., 1998. NaCl aerosol particle hygroscopicity dependence on mixing with organic compounds. J. Atmos. Chem. 31, 321–346.

Ibrahim, S., Romanias, M.N., Alleman, L.Y., Zeineddine, M.N., Angeli, G.K., Trikalitis, P.N., et al., 2018. Water interaction with mineral dust aerosol: particle size and hygroscopic properties of dust. ACS Earth Space Chem. 2, 376–386.

Jaegle, L., Quinn, P.K., Bates, T.S., Alexander, B., Lin, J.T., 2011. Global distribution of sea salt aerosols: new constraints from in situ and remote sensing observations. Atmos. Chem. Phys. 11, 3137–3157.

Jia, X.H., Gu, W.J., Li, Y.J., Cheng, P., Tang, Y.J., Guo, L.Y., et al., 2018. Phase transitions and hygroscopic growth of $Mg(ClO_4)_2$, $NaClO_4$, and $NaClO_4$ center dot H_2O: implications for the stability of aqueous water in hyperarid environments on mars and on earth. ACS Earth Space Chem. 2, 159–167.

Jing, B., Wang, Z., Tan, F., Guo, Y.C., Tong, S.R., Wang, W.G., et al., 2018. Hygroscopic behavior of atmospheric aerosols containing nitrate salts and water-soluble organic acids. Atmos. Chem. Phys. 18, 5115–5127.

Karydis, V.A., Tsimpidi, A.P., Bacer, S., Pozzer, A., Nenes, A., Lelieveld, J., 2017. Global impact of mineral dust on cloud droplet number concentration. Atmos. Chem. Phys. 17, 5601–5621.

Koehler, K.A., Kreidenweis, S.M., DeMott, P.J., Prenni, A.J., Petters, M.D., 2007. Potential impact of Owens (dry) Lake dust on warm and cold cloud formation. J. Geophys. Res. Atmos. 112, D12210.

Kumar, P., Sokolik, I.N., Nenes, A., 2011. Measurements of cloud condensation nuclei activity and droplet activation kinetics of fresh unprocessed regional dust samples and minerals. Atmos. Chem. Phys. 11, 3527–3541.

Lamb, D., Moyle, A.M., Brune, W.H., 1996. The environmental control of individual aqueous particles in a cubic electrodynamic levitation system. Aerosol Sci. Technol. 24, 263–278.

Lee, C.T., Chang, S.Y., 2002. A GC-TCD method for measuring the liquid water mass of collected aerosols. Atmos. Environ. 36, 1883–1894.

Lee, C.T., Hsu, W.C., 1998. A novel method to measure aerosol water mass. J. Aerosol Sci. 29, 827–837.

Lee, C.T., Hsu, W.C., 2000. The measurement of liquid water mass associated with collected hygroscopic particles. J. Aerosol Sci. 31, 189–197.

Li, X., Gupta, D., Eom, H.J., Kim, H., Ro, C.U., 2014. Deliquescence and efflorescence behavior of individual NaCl and KCl mixture aerosol particles. Atmos. Environ. 82, 36–43.

Li, Y.J., Liu, P.F., Bergoend, C., Bateman, A.P., Martin, S.T., 2017. Rebounding hygroscopic inorganic aerosol particles: liquids, gels, and hydrates. Aerosol Sci. Technol. 51, 388–396.

Liu, Y., Yang, Z.W., Desyaterik, Y., Gassman, P.L., Wang, H., Laskin, A., et al. , 2008. Hygroscopic behavior of substrate-deposited particles studied by micro-FT-IR spectroscopy and complementary methods of particle analysis. Anal. Chem. 80, 7179–7179.

Martin, S.T., 2000. Phase transitions of aqueous atmospheric particles. Chem. Rev. 100, 3403–3453.

Nenes, A., Pandis, S.N., Pilinis, C., 1998. ISORROPIA: a new thermodynamic equilibrium model for multiphase multicomponent inorganic aerosols. Aquat. Geochem. 4, 123–152.

ODowd, C.D., Smith, M.H., Consterdine, I.E., Lowe, J.A., 1997. Marine aerosol, sea-salt, and the marine sulphur cycle: a short review. Atmos. Environ. 31, 73–80.

Prather, K.A., Bertram, T.H., Grassian, V.H., Deane, G.B., Stokes, M.D., DeMott, P.J., et al., 2013. Bringing the ocean into the laboratory to probe the chemical complexity of sea spray aerosol. Proc. Natl. Acad. Sci. U.S.A. 110, 7550–7555.

Richardson, C.B., Snyder, T.D., 1994. A study of heterogeneous nucleation in aqueous-solutions. Langmuir 10, 2462–2465.

Schindelholz, E., Tsui, L.K., Kelly, R.G., 2014. Hygroscopic particle behavior studied by interdigitated array microelectrode impedance sensors. J. Phys. Chem. A 118, 167–177.

Sullivan, R.C., Moore, M.J.K., Petters, M.D., Kreidenweis, S.M., Roberts, G.C., Prather, K.A., 2009. Effect of chemical mixing state on the hygroscopicity and cloud nucleation properties of calcium mineral dust particles. Atmos. Chem. Phys. 9, 3303–3316.

Tang, I.N., Fung, K.H., Imre, D.G., Munkelwitz, H.R., 1995. Phase-transformation and metastability of hygroscopic microparticles. Aerosol Sci. Technol. 23, 443–453.

Tang, I.N., Munkelwitz, H.R., 1994. Water activities, densities, and refractive-indexes of aqueous sulfates and sodium-nitrate droplets of atmospheric importance. J. Geophys. Res. Atmos. 99, 18801–18808.

Tang, M.J., Cziczo, D.J., Grassian, V.H., 2016. Interactions of water with mineral dust aerosol: water adsorption, hygroscopicity, cloud condensation, and ice nucleation. Chem. Rev. 116, 4205–4259.

Tang, M.J., Huang, X., Lu, K.D., Ge, M.F., Li, Y.J., Cheng, P., et al., 2017. Heterogeneous reactions of mineral dust aerosol: implications for tropospheric oxidation capacity. Atmos. Chem. Phys. 17, 11727–11777.

Tang, M., Chan, C.K., Li, Y.J., Su, H., Ma, Q., Wu, Z., et al., 2019a. A review of experimental techniques for aerosol hygroscopicity studies. Atmos. Chem. Phys. 19, 12631–12686.

Tang, M.J., Guo, L.Y., Bai, Y., Huang, R.J., Wu, Z., Wang, Z., et al., 2019b. Impacts of methanesulfonate on the cloud condensation nucleation activity of sea salt aerosol. Atmos. Environ. 201, 13–17.

Tang, M.J., Zhang, H., Gu, W., Gao, J., Jian, X., Shi, G., et al., 2019c. Hygroscopic properties of saline mineral dust from different regions in China: geographical variations, compositional dependence and atmospheric implications. J. Geophys. Res. Atmos. 124, 10844–10857.

Wang, H., Wang, X.F., Yang, X., Li, W.J., Xue, L.K., Wang, T., et al., 2017. Mixed chloride aerosols and their atmospheric implications: a review. Aerosol Air Qual. Res. 17, 878–887.

Wexler, A.S., Seinfeld, J.H., 1991. Second-generation inorganic aerosol model. Atmos. Environ. Part A 25, 2731–2748.

Zieger, P., Vaisanen, O., Corbin, J.C., Partridge, D.G., Bastelberger, S., Mousavi-Fard, M., et al., 2017. Revising the hygroscopicity of inorganic sea salt particles. Nat. Commun. 8, 15883.